Definition and Evaluation of Mean Beam Lengths for Applications in Multidimensional Radiative Heat Transfer: A Mathematically Self-Consistent Approach

Walter W. Yuen
Department of Mechanical Engineering,
University of California at Santa Barbara,
Santa Barbara, CA 93106

A set of mathematically self-consistent definitions of mean beam length is introduced to account for surface-surface, surface-volume, and volume-volume radiative exchanges in general three-dimensional inhomogeneous medium. Based on these definitions, the generic exchange factor (GEF) formulated by the recently introduced multiple-absorption-coefficient-zonal-method (MACZM) can be written in an equivalent one-dimensional form. The functional behavior of the proposed mean beam lengths is shown to be readily correlated by either simple algebraic relations or neural network based correlations. They can be implemented directly with MACZM in general computational code to account for the radiation effect in complex three-dimensional systems. In addition, these definitions of mean beam length can also be used to assess the accuracy of the conventional mean beam length concept currently used by the practicing engineering community. [DOI: 10.1115/1.2969752]

Introduction

The concept of mean beam length (MBL) was originally formulated by Hottel [1,2] over 50 years ago. It was introduced as a length scale to account for the effect of geometry in the evaluation of radiative heat transfer between an isothermal gas volume and its boundary. Specifically, if $q_{\lambda i,k}$ is the radiative heat flux incident on a surface A_k from a radiating volume V with A_k being all or a part of its boundary, the traditional definition of the MBL, L_e, is defined as

$$q_{\lambda i,k} = (1 - e^{a_\lambda L_e}) e_{\lambda b,g} \tag{1}$$

where $e_{\lambda b,g}$ is the blackbody emissive power evaluated at a specific wavelength and the medium's temperature and a_λ is the corresponding absorption coefficient. Physically, MBL can be interpreted as the required radius of an equivalent hemisphere of a medium such that the flux received by the center of its base is equal to the average flux radiated to the area of interest by the actual volume of the medium.

For an isothermal nongray gas volume with arbitrary optical thickness, a number of works were reported [3–6] suggesting that the "exact" MBL can be approximated by

$$L_e = C L_{e,0} \tag{2}$$

where C is estimated to be in the range 0.8–1.0, and $L_{e,0}$ is the optically thin limit of the MBL given by

$$L_{e,0} = \frac{4V}{A} \tag{3}$$

with V and A being the volume and boundary of the medium, respectively. The applicability of Eq. (2) for isothermal media has been verified for different geometric configurations [7,8].

For radiative heat transfer in inhomogeneous, nonisothermal, and nongray media, However, the MBL concept is generally not applicable mathematically. But due to the difficulty in performing accurate multidimensional nongray calculation, Eq. (2) is still widely used by many engineering designers and commercially available computational fluid dynamics (CFD) codes as a basis to estimate the multidimensional effect of thermal radiation. This approach, however, is generally done without mathematical validation and it has led to much uncertainty in determining the importance of radiative heat transfer effect in practical engineering application scenarios. The objective of this work is to develop a more general set of length scales, which are mathematically correct and physically consistent in application for general radiative heat transfer.

Based on the generic exchange factor (GEF) concept introduced by the recently developed multiple-absorption-coefficient-zonal-method (MACZM) [9], the present work will show that six separate independent definitions of the MBL (two transmission MBLs, two emission MBLs, and two absorption MBLs) are needed to characterize the transmission, emission, and absorption processes of general three-dimensional radiative exchange. Simple correlations of the six MBLs are generated. The two transmission MBLs are shown to have simple functional behavior and can be readily correlated with a simple algebraic expression. The two absorption MBLs are shown to be effectively equivalent to the two emission MBLs. The two emission MBLs have complex functional behavior. However, they can be correlated by simple algebraic expressions generated by neural network.

In addition to serve as length scales for the various radiative heat transfer processes, the six correlated MBLs reduce the surface-surface, volume-surface, and volume-volume GEFs to simple 1D expressions. These MBL correlations eliminate the need to evaluate GEFs numerically in an actual calculation and MACZM can thus be implemented accurately and efficiently in CFD codes.

Concepts of GEF and the Basic Geometry

In the formulation of the MACZM [9], the three basic radiative exchange processes (surface-surface, surface-volume, and volume-volume) are shown to be characterized completely by three two-component GEFs, $s_1 s_{2,pp}$ $s_1 s_{2,pd}$; $g_1 s_{2,pp}$, $g_1 s_{2,pd}$; $g_1 g_{2,pp}$ and $g_1 g_{2,pp}$ and $g_1 g_{2,pd}$. As shown in Ref. [9], the radiative exchange between arbitrary volumes and surfaces in a three-dimensional inhomogeneous nonisothermal medium can be generated based on the superposition of these GEFs.

In the definition of GEFs, the emitting volume (surface) $V_1(A_1)$ and the absorbing volume (surface) $V_2(A_2)$ and their relative geometry are shown in Fig. 1. For the parallel (pp) component, A_1 is a square area with dimension D parallel to the x-y plane situated at the $z=0$ plane with one corner at the origin while V_1 is a cubical volume with dimension D and A_1 being its top surface area. For the perpendicular (pd) component, A_1 is a square area with dimension D parallel to the y-z plane situated at the $x=0$ plane with one corner at the origin while V_1 is a cubical volume with dimension D and A_1 being its surface area on the right. For all six GEFs, the absorbing area A_2 is a square area with dimension D parallel to the x-y plane and the absorbing volume V_2 is a cubical volume with dimension D and A_2 being its bottom surface. The position of the absorbing volume (area) $V_2(A_2)$ related to A_1 is specified by the coordinate at its lower left corner ($n_x D$, $n_y D$, $n_z D$) as shown in Fig. 1.

Contributed by the Heat Transfer Division of ASME for publication in the JOURNAL OF HEAT TRANSFER. Manuscript received June 19, 2007; final manuscript received June 4, 2008; published online September 5, 2008. Review conducted by Jayathi Murthy.

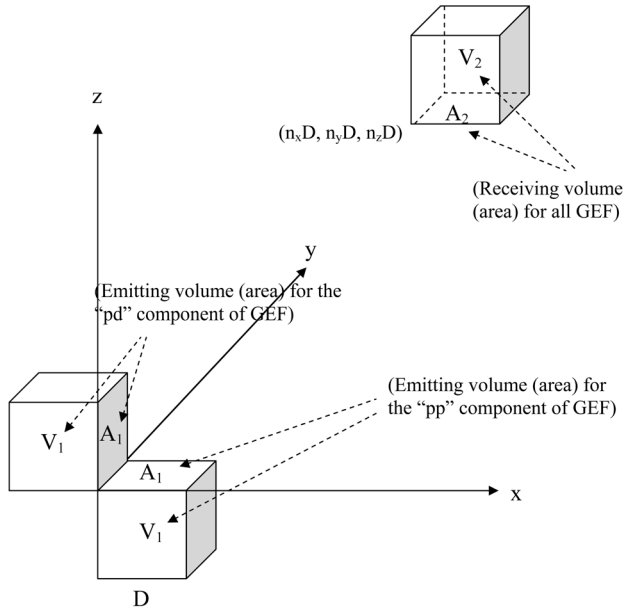

Fig. 1 Geometry of the emitting volume (area) and receiving volume (element) used in the definition of the two components of the GEF and the associated coordinate system

Mathematically, the two surface-surface GEFs $s_1s_{2,pp}$ and $s_1s_{2,pd}$ correspond to the actual exchange factors between the two square surfaces A_1 and A_2. For the four volume-surface and volume-volume GEFs $g_1s_{2,pp}$, $g_1g_{2,pd}$, $g_1g_{2,pp}$ and $g_1s_{2,pd}$, the exchange factors include only the portion of the radiation emitted by V_1 through the surface A_1. For the two volume-volume GEFs $g_1g_{2,pp}$ and $g_1g_{2,pd}$, the exchange factor is further limited by including only the radiation received by the volume V_2 through the surface A_2.

Actual volume-surface and volume-volume exchange factors are generated from the six GEFs by superposition. The detail of the superposition is presented in Ref. [9] and will not be repeated here. It should be noted that by restricting the emission/absorption through specific areas in the definition of the three basic GEFs, the MACZM approach can simulate accurately the variation of optical properties in an inhomogeneous medium, particularly in a region of large discontinuity in optical properties (e.g. a continuously changing 3D solid/liquid/gas phase boundary). The six GEFs are the basis for the definition of six corresponding MBLs in the present work.

The Concepts of Transmission, Absorption, and Emission Mean Beam Length

Mathematically, the two surface-surface GEFs $s_1s_{2,pp}$ and $s_1s_{2,pd}$, normalized by the area D^2, depend only on the optical thickness, and the relative orientation between the two areas as specified by (n_x, n_y, n_z). The optical thickness τ_{12} is evaluated along the line of sight between the center-point of the two areas. The two transmission MBLs are defined by

$$\frac{s_1s_{2,xx}}{D^2} = F_{12,xx}(n_x,n_y,n_z)e^{-a_mL_{t,xx}}, \quad xx = pp,pd \tag{4}$$

In the above expressions, $F_{12,xx}(n_x,n_y,n_z)$, $xx=pp,pd$ are the view factors between the two areas for the two configurations. The average absorption coefficient between the two surfaces, a_m, is

$$a_m = \frac{\tau_{12}}{L_c} \tag{5}$$

with L_c being the distance between the center of the two surfaces.

The concept of emission MBL is introduced based on the volume-surface exchange process characterized by the two GEFs, $g_1s_{2,pp}$ and $g_2s_{2,pd}$, with the emitting volume V_1 and absorbing area A_2 as shown in Fig. 1. As an extension to Eq. (4), the emission MBLs for the two configurations are defined by

$$\frac{g_1s_{2,xx}}{D^2} = F_{12,xx}(n_x,n_y,n_z)(1-e^{-a_1L_{\mathrm{em},xx}})e^{-a_mL_{t,xx}}, \quad xx = pp,pd \tag{6}$$

where a_1 is the absorption coefficient of the emitting medium in volume V_1. The two emission MBLs $L_{\mathrm{em},pp}$ and $L_{\mathrm{em},pd}$ are functions of the two absorption coefficients a_1 and a_m, as well as the geometrical configuration represented by (n_x, n_y, n_z).

Finally, the concept of absorption MBL is introduced based on the volume-volume exchange GEFs $g_1g_{2,pp}$ and $g_1g_{2,pd}$, with the emitting volume V_1 and absorbing volume V_2 as shown in Fig. 1. Generalizing the mathematical expression introduced by Eq. (6), the absorption MBLs for the two components are given by

$$\frac{g_1g_{2,xx}}{D^2} = F_{12,xx}(n_x,n_y,n_z)(1-e^{-a_1L_{\mathrm{em},xx}})(1-e^{-a_2L_{a,xx}})e^{-a_mL_{t,xx}}, \quad xx = pp,pd \tag{7}$$

where a_2 is the absorption coefficient of the medium in volume V_2. The two absorption MBLs $L_{a,pp}$ and $L_{a,pd}$ are functions of the three absorption coefficients a_1, a_2, and a_m, as well as the geometrical configuration represented by (n_x, n_y, n_z).

It is important to note that, together, the three MBLs (absorption, emission, and transmission MBLs) in its two-component are a set of path lengths, which reduce the six GEFs to equivalent one-dimensional expressions (Eqs. (4), (6), and (7)). Since these path lengths are introduced to account for the three distinct physical processes, their mathematical behaviors are influenced most strongly by the absorption coefficient associated with the specific process. The geometric effect is largely accounted for by the view factor and, therefore, the dependence of the MBLs on (n_x, n_y, n_z) is generally weak. The one-dimensional form of the GEFs can potentially serve as a basis for further development of additional engineering correlation to account for the nongray effect of multidimensional radiative heat transfer.

The Transmission Mean Beam Length, $L_{t,pp}$ and $L_{t,pd}$

Numerical data show that for two disjoint surfaces, the two transmission MBLs $L_{t,pp}$ and $L_{t,pd}$ are generally independent of optical thickness and can be approximated accurately by the corresponding center-to-center distances $L_{c,pp}$ and $L_{c,pp}$. One exception is that the pd component with $(n_x,n_y,n_z)=(0,0,1)$, when A_1 and A_2 are two perpendicular square surfaces with a common edge. For this case, the transmission MBL can be correlated by

$$\frac{L_{t,pd}}{L_{c,pd}} = 0.78 - 012\tau_{12} + 0.0093\tau_{12}^2 \quad (n_x,n_y,n_z) = (0,0,1) \tag{8}$$

The Emission Mean Beam Length $L_{\mathrm{em},pp}$ and $L_{\mathrm{em},pd}$

Physically, the behavior of the emission MBL for the case with the absorbing surface in contact with the emitting volume (the pp component with $(n_x,n_y,n_z)=(0,0,0)$) is expected to differ from cases in which the absorbing area and the emitting volume are disjoint. Different correlations are thus needed for the two possibilities. Specifically, the GEF $g_1s_{2,pp}$ with $(n_x,n_y,n_z)=(0,0,0)$ corresponds to the actual exchange factor between a cubical volume and one of its bounding surface. The transmission MBL is zero. The emission MBL is tabulated and shown in Fig. 2(*a*). The conventional MBL, given by Eq. (2) with $C=0.9$, is shown in the same figure for comparison. The corresponding prediction for the exchange factor is shown in Fig. 2(*b*). The conventional MBL is clearly not an accurate approximation of the emission MBL. The

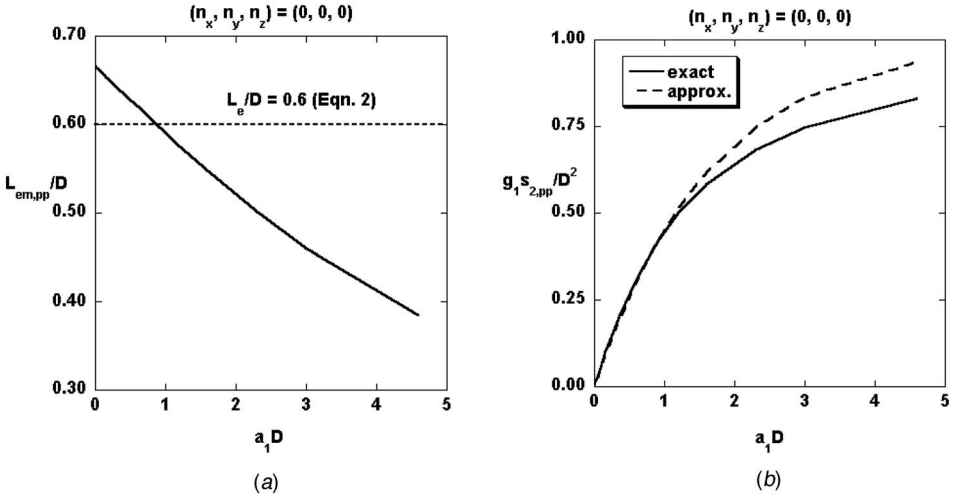

Fig. 2 Comparison of the emission MBL and the conventional MBL and the corresponding exchange factor for the $g_1 g_{2,pp}$ exchange factor with $(n_x, n_y, n_z)=(0,0,0)$

discrepancy in the exchange factor prediction is large in the limit of an optically thick emitting volume (i.e., large $a_1 D$). The numerical data presented in Fig. 2(a) can be correlated by

$$\frac{L_{\mathrm{em},pp}(0,0,0)}{D} = 0.67 - 0.081 a_1 D + 0.0043 (a_1 D)^2 \tag{9}$$

For cases in which the emitting volume and the absorbing area are disjoint, the emission MBLs are influenced strongly by the two optical thicknesses $a_1 D$ and τ_{12} and geometry (n_x, n_y, n_z). Since algebraic correlations are difficult to obtain, a neural network is created to provide a simple mathematical correlation. The capability of using neural networks to correlate experimental or numerical data accurately is well documented [10]. Specifically, using a two-layer neural network as shown in Fig. 3, neural network correlations are developed for the two emission MBLs. For $L_{\mathrm{em},pp}$ in ranges of $0 \le n_x \le 7$, $0 \le n_y \le 7$, $1 \le n_z \le 7$, $0.01 \le a_1 D \le 4.6$, and $0 \le \tau_{12} \le 4.6$, the numerical data can be correlated with the following equation:

$$z = \sum_{i=1}^{18} \left\{ \tanh\left[\left(\sum_{j=1}^{5} W_{1,ij} p_j \right) + b_{1,i} \right] \right\} W_{2,i} + b_2 \tag{10}$$

where $\boldsymbol{p}$ is a normalized input vector with components $\bar{n}_x$, $\bar{n}_y$, $\bar{n}_z$, $\overline{a_1 D}$, and $\bar{\tau}_{12}$ and $z = \overline{L_{\mathrm{em},pp}/L_{c,pp}}$ is the normalized output. All normalized variables are generated by a linear transformation from its range of value to the common range of -1 to 1. Numerical values for the network elements $\hat{W}_1$, $\boldsymbol{b}_1$, $\boldsymbol{W}_2$, and b_2 are available upon request to the author. The accuracy of the neural network prediction is illustrated for some typical data with $n_z=1$ in Fig. 4. The conventional MBL, given by Eq. (2) with $C=0.9$, is shown in the same figure to demonstrate the general inaccuracy of the conventional MBL concept.

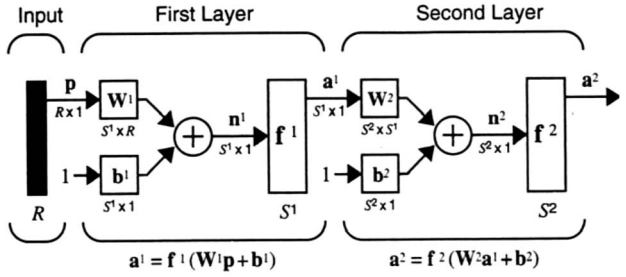

Fig. 3 Schematic of a two-layer neural network used in generating the correlation for the emission MBL

Because of the more complex mathematical behavior of $L_{\mathrm{em},pd}$, two separate neural network correlations are generated to simulate the numerical data. For $0 \le n_x \le 5$, $1 \le n_z \le 7$, $0.01 \le a_1 D \le 4.6$, and $0 \le \tau_{12} \le 4.6$ with $n_y=0$, the data are correlated by the following equation:

$$z = \sum_{i=1}^{13} \left\{ F\left[\left(\sum_{j=1}^{4} W_{1,ij} p_j \right) + b_{1,i} \right] \right\} W_{2,i} + b_2 \tag{11}$$

with

$$F(x) = \frac{1}{1+e^{-x}} \tag{12}$$

The normalized vector $\mathbf{p}$ is a vector with components $\bar{n}_x$, $\bar{n}_z$, $\overline{a_1 D}$, and $\bar{\tau}_{12}$ Note that $z = \overline{L_{\mathrm{em},pd}/L_{c,pd}}$ is normalized to be within the range 0–1, which is the range of the "log-sigmoid" transfer function as represented by Eq. (12).

For cases with $1 \le n_y \le 6$, a second network is generated to correlate the numerical data as follows:

$$z = \sum_{i=1}^{21} \left\{ F\left[\left(\sum_{j=1}^{5} W_{1,ij} p_j \right) + b_{1,i} \right] \right\} W_{2,i} + b_2 \tag{13}$$

with $\boldsymbol{p} = (\bar{n}_x, \bar{n}_y, \bar{n}_z, \overline{a_1 D}, \bar{\tau}_{12})$. Detailed numerical data of the two networks are available upon request to the author. The accuracies of the two neural network correlations are illustrated for some selected geometry with $n_z=1$ in Fig. 5. The conventional MBL, given by Eq. (2) with $C=0.9$, is again shown in the same figure to demonstrate the inaccuracy of the conventional MBL concept.

It should be noted that the numerical data and the associated neural network correlation for the emission MBLs $L_{\mathrm{em},pp}$ and $L_{\mathrm{em},pd}$ are generated only for a finite range of the input variables $a_1 D$, τ_{12}, n_x, n_y, and n_z. Since the emitting volume is expected to approach a blackbody in the limit of a large emission optical thickness ($a_1 D$) and GEF is generally small (approaches zero) in the limit of a large distance between the emitting volume and the absorbing surface, the accuracy of the emission MBL is less critical in those limits. For the optically thick limit $a_1 D > 4.6$ and/or $\tau_{12} > 4.6$, it is sufficient to use the corresponding emission MBL evaluated at $a_1 D = 4.6$ and/or $\tau_{12} = 4.6$. For a geometric configura-

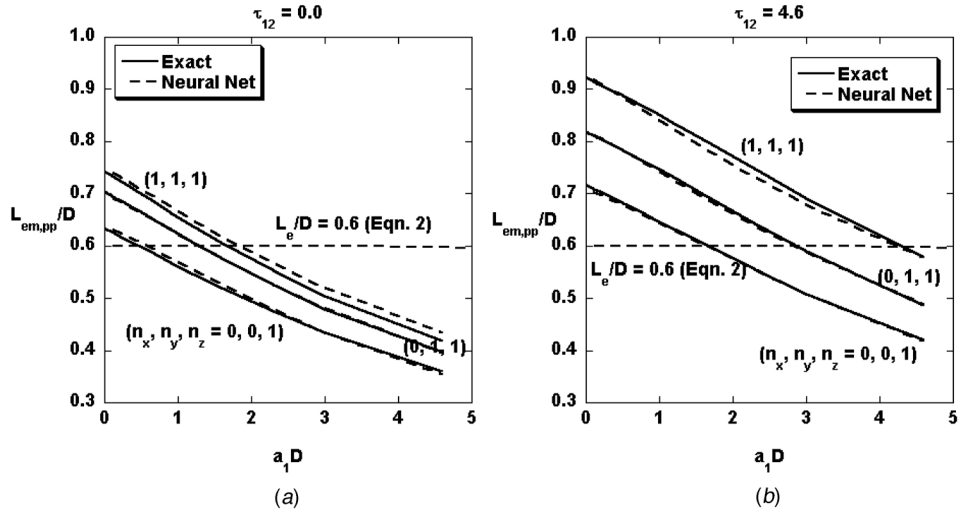

Fig. 4 Comparison between the neural network prediction of the emission MBL, $L_{em,pp}$, for different geometric configurations with n_z=1

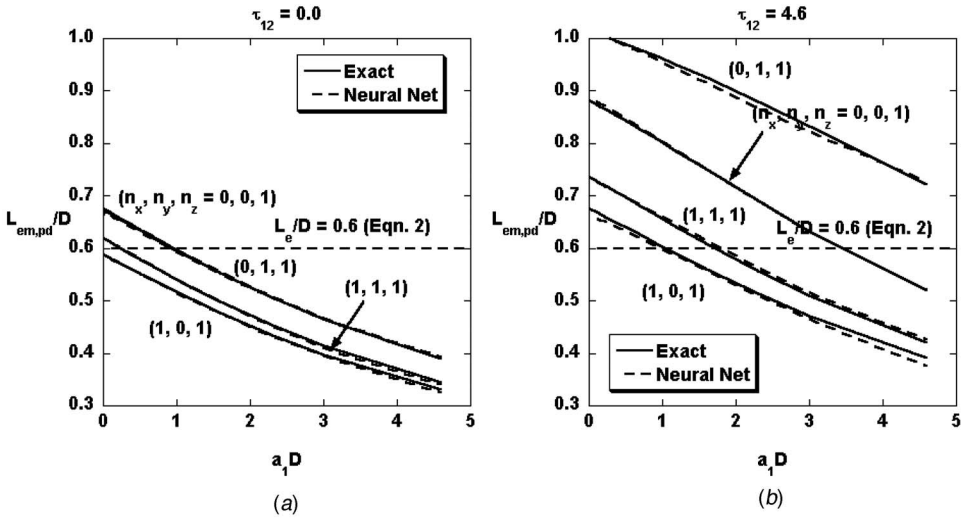

Fig. 5 Comparison between the neural network prediction of the emission MBL, $L_{em,pd}$, for different geometric configurations with n_z=1

tion with (n_x, n_y, n_z) outside of the specified range, the normalized emission MBL can be taken to be the value evaluated at a configuration with the closest distance.

Absorption Meam Beam Length, $L_{a,pp}$ and $L_{a,pd}$

Numerical data show that, in general, the absorption MBL is effectively independent of the optical properties of the emitting volume and can be taken to be the same as the emission MBL evaluated at the optical property of the absorbing volume. Due to the selection of the x-direction as the orientation of A_1 in the definition of the pd component of the GEF, the equivalence between the pd component of the absorption MBL and the mission MBL would require an exchange in the value of n_x and n_z as follows:

$$L_{a,pp}(n_x,n_y,n_z,a_1D,a_2D,\tau_{12}) = L_{\mathrm{em},pp}(n_x,n_y,n_z,a_2D,\tau_{12}) \tag{14a}$$

$$L_{a,pd}(n_x,n_y,n_z,a_1D,a_2D,\tau_{12}) = L_{\mathrm{em},pd}(n_x-1,n_y,n_x+1,a_2D,\tau_{12}) \tag{14b}$$

Nomenclature

- a_1 = absorption coefficient of the emitting volume V_1
- a_2 = absorption coefficient of the absorbing volume V_2
- a_λ = absorption coefficient at wavelength λ
- a_m = average absorption coefficient of the medium between surfaces A_1 and A_2
- A = surface area
- C = constant used in the definition of the conventional mean beam length, Eq. (2)
- D = characteristic dimension used in the definition of GEF
- $e_{\lambda b}$ = blackbody emissive power

F_{ij} = view factor between surfaces A_i and A_j
$g_1 g_{2,xx}$ = the xx component of the volume-volume GEF, $xx=pp,pd$
$g_1 g_{2,xx}$ = the xx component of the volume-surface GEF, $xx=pp,pd$
L_e = conventional mean beam length introduced by Hottel
L_a = absorption mean beam length, Eq. (7)
L_{em} = emission mean beam length, Eq. (6)
L_c = center-to-center distance between surfaces A_1 and A_2
$L_{e,0}$ = optically thin limit of the conventional mean beam length, Eq. (3)
L_t = transmission mean beam length, Eq. (4)
n_x = discretized x-coordinate of A_2 relative to A_1 in the definition of GEF
n_y = discretized y-coordinate of A_2 relative to A_1 in the definition of GEF
n_z = discretized z-coordinate of A_2 relative to A_1 in the definition of GEF
$q_{\lambda i,k}$ = incident radiative heat flux on surface A_k
$s_1 s_{2,xx}$ = the xx component of the surface-surface GEF, $xx=pp,pd$
S = distance
V = volume

Greek Symbols

λ = wavelength
θ = angular coordinate
τ_{12} = optical thickness between areas A_1 and A_2

Subscripts

i = the ith volume (or surface)
pp = parallel component
pd = perpendicular component

References

[1] Hottel, H. C., 1954, "Radiant-Heat Transmission," *Heat Transmission*, 3rd ed., W. H. McAdams, ed., McGraw-Hill, New York, Chap. 4.
[2] Hottel, H. C., and Sarofim, A. F., 1967, *Radiative Transfer*, McGraw-Hill, New York.
[3] Olfe, D. B., 1961, "Mean Beam Length Calculations for Radiation From Non-Transparent Gases," J. Quant. Spectrosc. Radiat. Transf., **1**, pp. 169–176.
[4] Dunkle, R. V., 1964, "Geometric Mean Beam Lengths for Radiant Heat Transfer Calculations," ASME J. Heat Transfer, **86**(1), pp. 75–80.
[5] Tien, C. L., and Wang, L. S., 1965, "On the Calculation of Mean Beam Length for a Radiating Gas," J. Quant. Spectrosc. Radiat. Transf., **5**, pp. 453–456.
[6] Mandell, D. A., and Miller, F. A., 1973, "Comparison of Exact and Mean Beam Length Results for a Radiating Hydrogen Plasma," J. Quant. Spectrosc. Radiat. Transf., **13**, pp. 49–56.
[7] Wassal, A. T., and Edwards, D. K.,1976, "Mean Beam Lengths for Spheres and Cylinders," ASME J. Heat Transfer, **98**, pp. 308–309.
[8] Anderson, K. M., and Hadvig, S., 1989, "Geometric Mean Beam Lengths for a Space Between Two Coaxial Cylinders," ASME J. Heat Transfer, **111**(3), pp. 811–813.
[9] Yuen, W. W., 2006, "Development of a Multiple Absorption Coefficient Zonal Method for Application to Radiative Heat Transfer in Multi-Dimensional Inhomogeneous Non-Gray Media," Numer. Heat Transfer, Part B, **49**(2), pp. 89–103.
[10] Hornik, K. M., Stinchcombe, M., and White, H., 1989, "Multilayer Feedforward Networks are Universal Approximators," Neural Networks, **2**, pp. 359–366.